

Metabolic profiling using Fourier-transform ion-cyclotron-resonance mass spectrometry

Daisaku Ohta · Daisuke Shibata · Shigehiko Kanaya

Received: 22 August 2007 / Revised: 20 September 2007 / Accepted: 21 September 2007 / Published online: 6 October 2007
© Springer-Verlag 2007

Abstract With the aid of the extreme resolving power of Fourier-transform ion-cyclotron-resonance mass spectrometry (FT-ICR/MS), we have developed a metabolomics platform for high-throughput metabolic profiling and metabolite candidate identification integrating a data-processing system, the Dr.DMASS program (<http://kanaya.naist.jp/DrDMASS/>), and a metabolite-species database, KNApSAcK (<http://kanaya.aist-nara.ac.jp/KNApSAcK/>). We discuss the potential of this FT-ICR/MS-based metabolic profiling scheme as a general metabolomics tool by clarification of plant metabolic disorders and specific metabolite accumulation patterns caused by herbicidal enzyme inhibitors.

Keywords Fourier-transform ion-cyclotron-resonance mass spectrometry · Metabolomics · Data processing

Introduction

Metabolomics targets enormous numbers of organic compounds of unknown structure [1–3]. This is an extreme

challenge in analytical chemistry when nearly infinite numbers of unknown natural compounds with different properties need to be addressed simultaneously. Thus, metabolomics platforms are classified according to the research objectives as well as the target organisms. For example, prototrophs including humans, which acquire nutrition from other organisms, synthesize only a limited variety of endogenous metabolites. Therefore, cutting-edge metabolomics for drug discovery needs to guarantee reliable/reproducible analytical platforms for metabolite identification and absolute quantification of a set of endogenous human metabolites. A broad range of excellent mass spectrometry (MS) systems with separation steps such as liquid or gas chromatography and capillary electrophoresis provides robust platforms for such metabolomics, focusing on the dynamics of human metabolism [4–6]. On the other hand, in metabolomics research such as nutritional chemistry and natural product chemistry, authentic metabolite samples are not easily accessible for comprehensive metabolomics, and additional means of analysis are necessary for acquisition of molecular information from a variety of unknown compounds. In this context, NMR is one of the good options for chemical structure studies and, in fact, NMR-based metabolomics studies have so far been widely applied [7–10].

Fourier-transform ion-cyclotron-resonance mass spectrometry (FT-ICR/MS) is a distinguished analytical method due to its extremely high resolution and sensitivity [11–14]. The high-resolving power allows direct infusion analyses of crude biological samples without chromatographic separation steps and derivatization reactions, and high-throughput metabolic profiling studies are done through assignment of only one or a few molecular formulas to each single m/z value in the spectra. However, its application in the life sciences has been primarily oriented towards proteomics

D. Ohta (✉)
Graduate School of Life and Environmental Sciences,
Osaka Prefecture University,
Sakai 599-8531, Japan
e-mail: ohtad@bioinfo.osakafu-u.ac.jp

S. Kanaya
Graduate School of Information Science,
Nara Institute of Science and Technology,
Ikoma 630-0192, Japan

D. Shibata
Kazusa DNA Research Institute,
Kisarazu 292-0818, Japan

research, and FT-ICR/MS-based metabolomics is still undeveloped mainly due to the difficulties in processing of FT-ICR/MS data as metabolome information. On the other hand, several outstanding studies [15–18] have proven the potential of FT-ICR/MS as a unique metabolomics tool. Thus, development of a general scheme of FT-ICR/MS-based metabolic profiling, with the aid of its potential for high-resolution power together with ion-signal intensity information, should make a significant contribution to metabolomics studies. In this report, we discuss the development of a metabolic profiling scheme based on FT-ICR/MS analysis furnished with a data-processing scheme (Dr.DMASS) and a metabolite-species relationship database (KNAPSAcK) for prediction of candidate metabolites [19, 20].

Analytical conditions

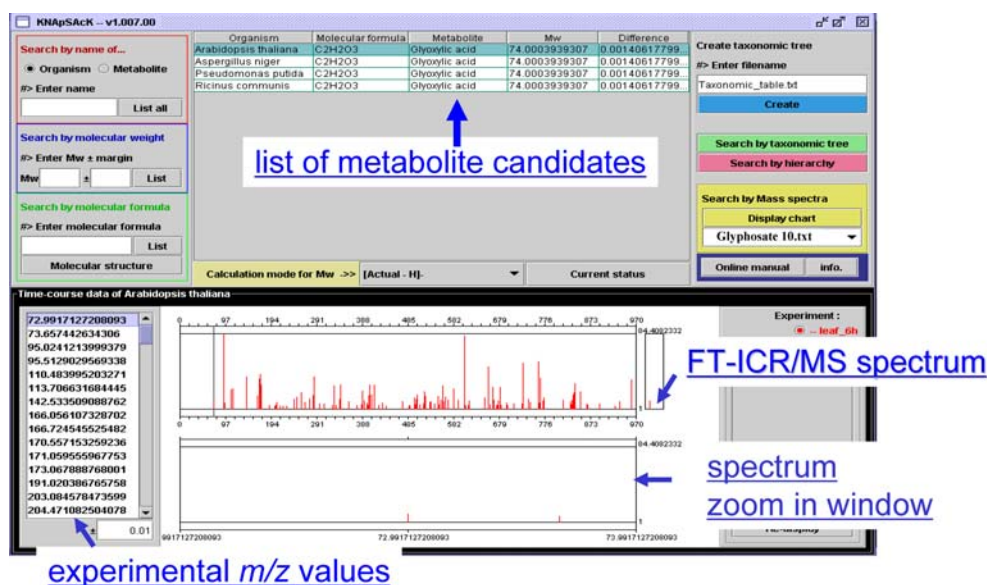
Metabolomics data were collected using an IonSpec Explorer FT-ICR/MS (IonSpec Inc., Lake Forest, CA, USA) with a 7-Tesla magnet. We set analytical conditions for reproducible detection of approximately 200–300 analytes from each tissue extract sample. Briefly, samples were infused using a Harvard syringe pump model 22 (Harvard Apparatus, Holliston, MA, USA) at a flow rate of 0.5 to 1.0 $\mu\text{L min}^{-1}$ through a 100- μL Hamilton syringe. The potentials on the electrospray emitters were set to 3.0 kV and -3.0 kV for the positive and the negative electrosprays, respectively. The base pressure in the source region was $\sim 5 \times 10^{-5}$ torr (1 torr = 133.3 Pa). Ionized metabolites were accumulated for a period of 2500 to 5000 milliseconds in a hexapole ion trap/guide and transferred through an RF-only quadrupole into the FT-ICR cell. The direct current potentials in the positive and negative ion mode analyses were, respectively, -2 V and 2 V during ion accumulation and 2 V and -2 V for ion transfer into the FT-ICR cell. In the positive and negative ion modes, the potentials on the extraction plate were, respectively, 12 V and -12 V during ion trapping and were reversed to -2 V and 2 V for extraction. The base pressure in the analyzer region was set to the level of $\sim 4 \times 10^{-10}$ torr. ESI-MS spectra were acquired over the m/z range 55 to 1000 from 1024×1024 independent data points. Under our analytical conditions the resolving power ($m/\Delta m_{50\%}$) was routinely about 100,000 (for $m/z=400$ with 1 s ion-accumulation time), and the mass accuracy was below 2 ppm. The high resolving power of FT-ICR/MS allows the separate detection of individual metabolites in crude biological samples without steps of chromatography and derivatization. Furthermore, elemental compositions of analytes can be estimated with the aid of accurate mass measurement leading to the prediction of possible metabolite candidates.

For the FT-ICR/MS analyses, we added internal mass calibrants (IMCs) to experimental samples for correcting the analytical errors in terms of m/z values. These IMCs were lidocaine, prochloraz, reserpine, and bombesin for positive ion mode analysis, and an IMC set of 2,4-dichlorophenoxyacetic acid, ampicillin, 3-[(3-cholamidopropyl)dimethylammonio]propanesulfonic acid, and tetra-*N*-acetylchitotetraose was used for negative ion mode analysis. The m/z correction was done in terms of the actual m/z values of these authentic IMC compounds, while endogenous metabolites could also be used for this purpose. We performed 10 successive spectral scans for each sample analysis, and further data processing was done using the Dr.DMASS software [19]. Briefly, in each spectral scan, experimental m/z values of the IMCs were corrected to their theoretical values for the calibration of entire spectral data, and for every analyte, its m/z value was calibrated using a linear relationship between theoretical and experimental values for the IMCs. Then, the calibrated m/z values of repeatedly identifiable analytes were automatically matched to one another among 10 spectral scans. After the calibration, deviations of m/z values of detected analytes converged to a molecular weight range of 0.001. The intensity values of reproducibly observed analytes were converted into percentage values of total ion intensity. Thus, metabolome data from a single biological sample consisted of averaged m/z values with intensity information from 10 spectral scans. We prepared at least triplicate samples for each experimental treatment, and the corresponding ions were identified and matched one to another among triplicate samples. The processed data were subjected to statistical analyses using the *t*-test and the Pearson's correlation coefficient for individual analytes [19]. Metabolome comparison was done using two multivariate analyses, principal-component analysis (PCA) and batch-learning self-organizing map (BL-SOM) for clarification of metabolomes according to metabolite accumulation profiles [16–18, 21, 22]. The data correction scheme has been described in detail [19], and the software is downloadable with detailed instructions at the following Web site: <http://kanaya.aist-nara.ac.jp/DrDMASS/>.

Metabolite-species database

The development of a metabolite-species database (KNAPSAcK, <http://kanaya.naist.jp/KNAPSAcK/>) has allowed high-throughput prediction of metabolite identities from FT-ICR/MS data [19]. A total of 34,149 metabolite-species pairs encompassing 16,529 metabolites and 8,557 species have so far been compiled from about 7,600 published references (February 16th, 2007) mainly covering plants and microbes. The database enabled a high-throughput search using FT-ICR/MS analysis data for metabolite-species relationships together with detailed metabolite information

Fig. 1 The main search window of the KNApSAcK database. After Dr.DMASS data processing, FT-ICR/MS spectral data can be uploaded to the KNApSAcK database, and metabolite candidates can be searched for every m/z value. A variety of metabolite search options are available for users. The database with instruction manuals is downloadable at <http://kanaya.naist.jp/KNApSAcK/>



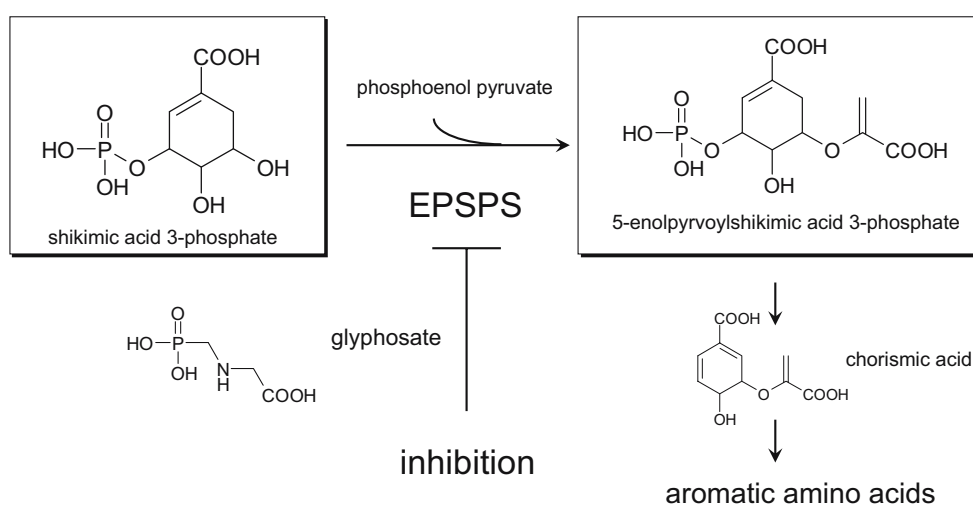
including molecular weight, molecular formula, chemical structures, CAS numbers, biological functions, and references of academic papers (Fig. 1). The KNApSAcK database has been designed to analyze FT-ICR/MS data sets after Dr. DMASS processing, and each accurate mass value can be attributed to only one or a very few molecular formulas leading to prediction of possible metabolite candidates. For metabolite prediction, the tolerance levels of m/z differences are freely changeable using a function on the KNApSAcK, and candidate metabolites with a predicted elemental composition are listed together with other possible candidates with closer molecular weight values. The database search can be performed focusing on formation of the ion adducts $[M + K]^+$, $[M + Na]^+$, $[M + NH_4]^+$, $[M + H]^+$, and $[M - H]^-$. Identification of true metabolite candidates is facilitated by narrowing down molecular formula possibilities incorporating information of intensity ratios of isotope ion peaks found in FT-ICR/MS spectra. Detailed instructions

with a demonstration are available (<http://kanaya.naist.jp/KNApSAcK/>).

Metabolic profiling

Aiming at metabolic profiling, the Dr.DMASS data-processing scheme was applied to differentiate plant metabolic disorders caused by chemical inhibition of the biosynthetic pathways of fatty acids, branched-chain amino acids, aromatic amino acids, and carotenoids [19]. Even under FT-ICR/MS conditions detecting 200–300 analytes from a single sample, the total number of analytes amounted to 1,560 from both positive and the negative ion mode analyses for treatments of specific enzyme inhibitions at different concentrations including EPSP synthase, acetolactate synthase, and acetyl-CoA carboxylase [19]. Out of the 1,560 analytes, a total of 518 were

Fig. 2 Inhibition of 5-enolpyruvylshikimic acid 3-phosphate synthase (EPSPS) by glyphosate. EPSPS catalyzes the reaction to yield 5-enolpyruvylshikimic acid 3-phosphate from shikimate 3-phosphate in the shikimate pathway leading to aromatic amino acid biosynthesis



found to be redundant among several different treatments, and their signal intensities increased or decreased with over twofold differences. The different signal intensities should be due to metabolic disorders caused by specific inhibition of different enzymatic steps. These results indicated that a specific set of metabolites built up, reflecting each specific enzyme inhibitor treatment. It should be noted that the variety of analytes and their abundances were not dramatically changed when tissue samples from normal growth conditions were compared [19]. We identified metabolite candidates for 284 analytes by searching the species–metabolite relationship database, KNApSAcK. Chemical structures of selected ions were confirmed by MS–MS analysis using the SORI-CID technique [19].

It is postulated that *Arabidopsis* may produce more than 5,000 compounds [23], and this metabolite profiling probably could have covered about 30% of the metabolites produced in this plant species. These results indicated that the FT-ICR/MS analytical condition for detecting 200–300 analytes was sufficient to differentiate plant metabolic disorders caused by specific enzyme inhibition [19].

Metabolomics data interpretation

We interpreted results from glyphosate treatment (1 week with 0, 1, 3, 10, 30, and 100 ppm) in an attempt to provide a generalization of FT-ICR/MS as a metabolomics research tool. Glyphosate is a specific inhibitor of 5-enolpyruvylshikimate-3-

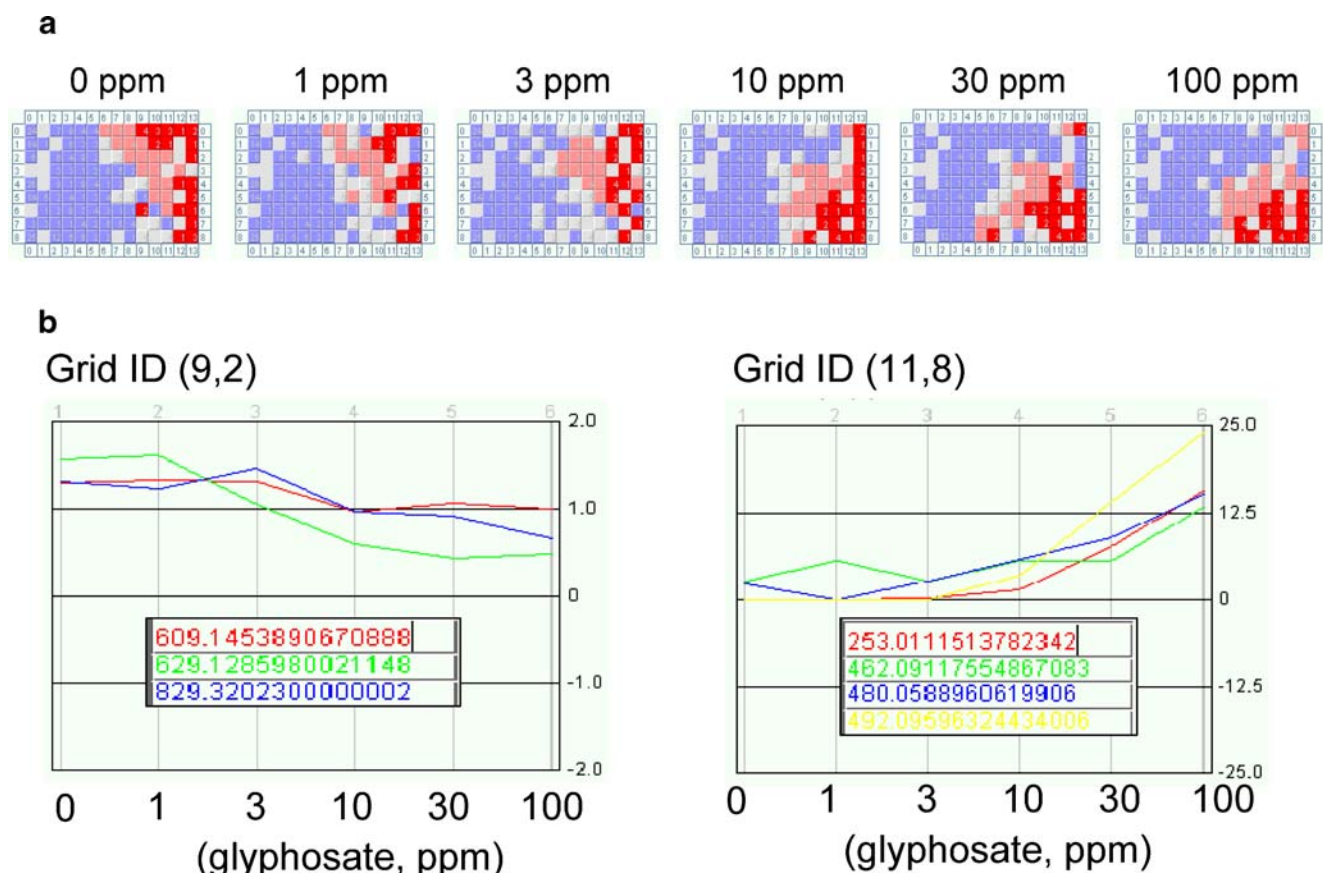


Fig. 3 BL-SOM (batch learning self organizing map) analyses after glyphosate treatment of *Arabidopsis thaliana* seedlings. *Arabidopsis* seedlings were treated with 0, 1, 3, 10, 30, and 100 ppm glyphosate for 1 week under sterile conditions and plant extracts were analyzed by the direct infusion FT-ICR/MS by the method described previously [19]. BL-SOM analyses were done using the Dr.DMASS program. In the BL-SOM, analytes were classified into groups (grids) accommodating similar decrease/increase patterns. In this experiment, the analyte groups were sorted into 104 different grids [13 (x-axis) × 8 (y-axis) = 104 grids] in each BL-SOM panel (0, 1, 3, 10, 30, and 100 ppm). On BL-SOM analysis the grid numbers should be adjusted in the Dr.DMASS program (<http://kanaya.aist-nara.ac.jp/DrDMASS/>) in proportion to the total data size. **(a)** Each of the six BL-SOM panels represents treatment with a different concentration (0, 1, 3, 10, 30, and 100 ppm) of glyphosate. Throughout the treatments (the six

BL-SOM panels), each grid contained the same set of analytes classified according to similar decrease/increase patterns. The *different colors* indicate variations of analyte numbers sorted into each grid (*blue* = few; *pink* = moderate; *red* = many). Grids of *gray color* contained no analytes. **(b)** Two examples of the contents of the grids. The examples on the *left* (from the grid of “9, 2” shown *upper left*) contained three analytes ($m/z=609.1453$, 629.1285 , and 829.3202) for which relative intensities decreased with increasing inhibitor concentrations. The examples on the *right* (from the grid “11, 8”) contained four analytes ($m/z=253.011$, 462.0911 , 483.0588 , and 492.0959) for which relative abundances increased when the inhibitor concentrations increased. The *inset* indicates the analytes (m/z) in each grid. The grid identities were defined using “x-axis number, y-axis number” as described above

phosphate synthase [24], which catalyzes the formation of 5-enolpyruvylshikimate-3-phosphate from shikimate 3-phosphate in the shikimate pathway en route to aromatic amino acid biosynthesis (Fig. 2). In this study, the glyphosate concentrations used were selected to include the IC_{50} (10 ppm), and, therefore, 30 and 100-ppm treatments seriously damaged the plants, eventually causing fatality [19]. Differentiation of metabolic profiles among the glyphosate treatments was apparent on the BL-SOM (Fig. 3), and metabolite accumulation patterns were classified by reference to the enzyme inhibitor concentrations shown in the six panels (Fig. 3).

Figure 4 shows the accumulation patterns of selected metabolite candidates in the glyphosate treatments. The levels of gluconasturtii, glucobrassin, and neoglucobrassin were clearly increased by the higher glyphosate concentrations, suggesting stimulation of glucosinolate biosynthesis in the inhibitor-treated plants. Also, fatty acids (palmitic acid and lauric acid) and phenylpropanoids (sinapic acid,

quercetin glucoside, and rhamnetin glucoside) levels were elevated by higher-concentration glyphosate treatments. Glutamine was maintained at relatively constant levels for the lower glyphosate concentrations but decreased dramatically after the 30 and 100-ppm treatments. Interestingly, the changes in glutamic acid levels were completely opposite to those in glutamine levels, suggesting facilitated conversion from glutamine to glutamic acid under the EPSPS inhibition conditions. The dynamic changes in the levels of glutamine and glutamic acid might be linked to the elevated glutathione levels (Fig. 4) in the glyphosate treatments. Further studies are necessary to clarify how the EPSPS inhibition caused the build-up of metabolites with no direct pathway interaction.

Changes in the glutathione levels (Fig. 4) in the glyphosate treatments were studied in detail in the presence of variable concentrations of aromatic amino acids, the pathway end-products (Fig. 5). The molecular identity of the ion (Fig. 4, $m/z=306.0752$) was confirmed as glutathione by MS–MS

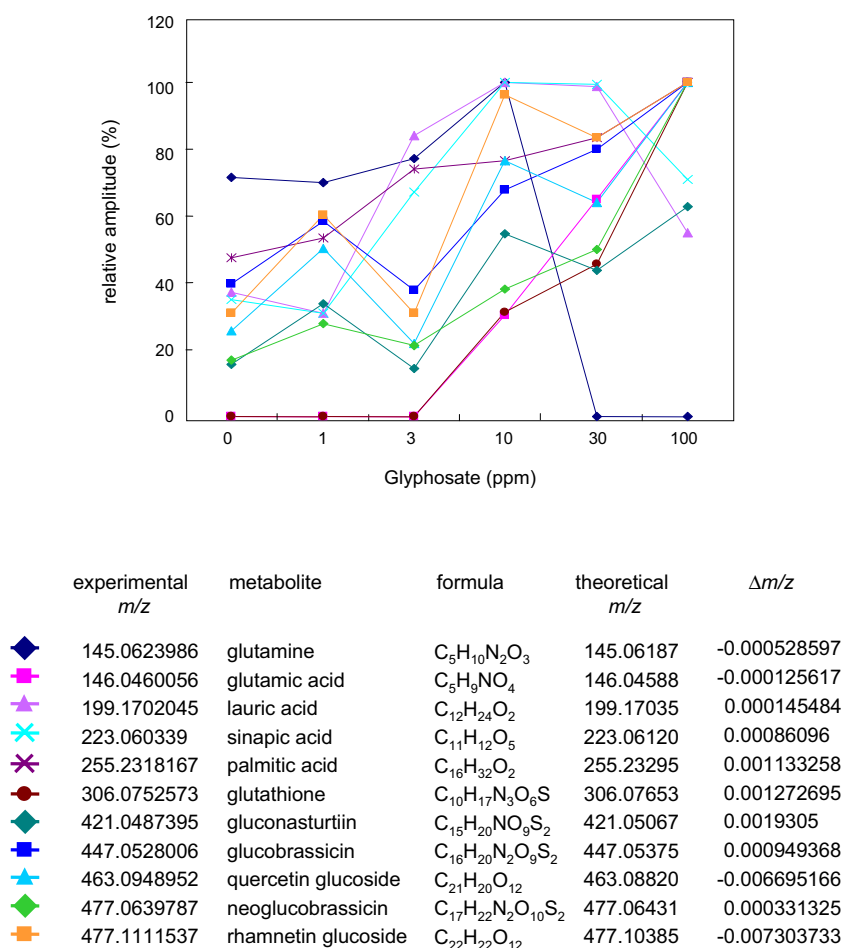


Fig. 4 Different patterns of accumulation of selected analytes in *Arabidopsis* seedlings as a result of treatment with different concentrations (0, 1, 3, 10, 30, and 100 ppm) of glyphosate. Changes in the levels of each metabolite among the glyphosate concentrations (0, 1,

3, 10, 30, and 100 ppm) were compared in terms of the relative values of their signal intensities (the highest intensity value observed for each ion = 100%)

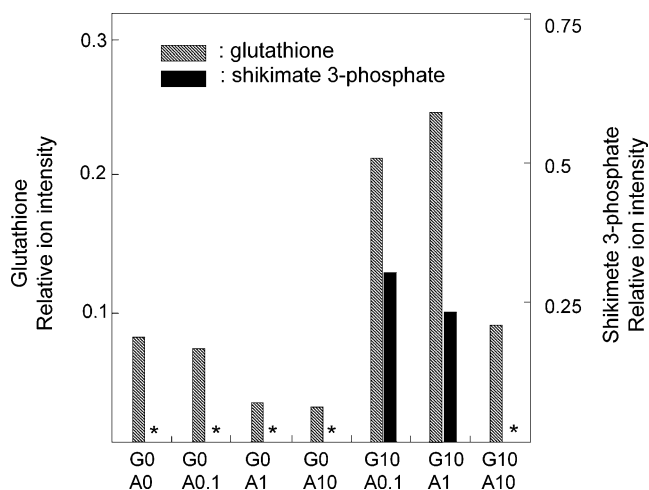


Fig. 5 Changes in glutathione and shikimate 3-phosphate levels in *Arabidopsis* seedlings treated with different concentrations of glyphosate with a mixture of aromatic amino acids. *G0A0* was the control experiment without both glyphosate and aromatic amino acids. The set *G0A0.1*, *G0A1*, and *G0A10* were treatments with different concentrations of aromatic amino acids (0.1, 1, 10 $\mu\text{mol L}^{-1}$) without glyphosate. With 10-ppm glyphosate, concentrations of aromatic amino acids (0.1, 1, 10 $\mu\text{mol L}^{-1}$) were also added (*G10A0.1*, *G10A1*, and *G10A10*). Aromatic amino acids (tryptophan, phenylalanine, and tyrosine), the pathway end-products (Fig. 2), were added at different concentrations (0.1, 1, 10 $\mu\text{mol L}^{-1}$). Asterisks indicate the treatments in which no corresponding ions were detected

analysis (not shown). In the one-week glyphosate treatments, both shikimate 3-phosphate ($m/z=253.0111$) and glutathione levels increased when the plants were treated with higher concentrations of the enzyme inhibitor (Figs. 4 and 5). Accumulation levels of shikimate 3-phosphate (Fig. 5), the enzyme substrate (Fig. 2), increased in accordance with glyphosate concentrations, which should correspond to the degree of enzyme inhibition.

In the 10-ppm glyphosate treatments, both the shikimate 3-phosphate levels and the glutathione levels were reduced by addition of a mixture of aromatic amino acids, suggesting that the damage caused by the enzyme inhibitor was alleviated by addition of the pathway end-products (Fig. 5). Smith [25] reported that glyphosate had no significant effect on glutathione levels during their short exposure period of several hours in barley (*Hordeum vulgare*), tobacco (*Nicotiana tabacum*), soybean (*Glycine max*), or corn (*Zea mays*). On the other hand, when the three groundnut cultivars JL24, CO2, and TMV2 were treated with glyphosate for longer periods, the activity of glutathione *S*-transferase and glutathione levels increased significantly in a dose-dependent manner [26]. Furthermore, glyphosate-tolerant cell lines of groundnut showed an elevated basal level of glutathione *S*-transferase activity and non-protein thiol content [26]. These results indicated that the EPSPS inhibition itself did not affect glutathione levels, reflecting highly selective enzyme inhibition by glyphosate.

It is known that glutathione is involved in stress and xenobiotics detoxification responses [27–29]. Taken together, our FT-ICR/MS metabolomics data agreed with previous findings, demonstrating that the metabolic profiling results could be evaluated in a biological context.

FT-ICR/MS as a general metabolomics tool

The excellent performance of FT-ICR/MS analysis has been repeatedly demonstrated by use of its ultra-high resolving power; low quantitative capability is an intrinsic weakness of FT-ICR/MS analysis, however. Particularly in direct infusion analyses with ESI-coupled FT-ICR/MS, the accuracy of quantitation is adversely affected by ion-suppression phenomenon in which compounds present in a complex mixture compete against other compounds in the ionization step.

Current results indicate that the metabolite accumulation patterns demonstrated by FT-ICR/MS could reflect physiological events. We designed our experiments to detect dose-dependent metabolic disorders caused by enzyme inhibitor treatments at differential concentrations. Thus, we were able to ascribe different metabolic profiles to the chemical treatments (inhibition of specific enzymatic steps) by studying dose-dependent metabolome patterns (changes in ion-intensity values). Monitoring temporal changes would also be crucial for linking metabolic profiling data to physiological events.

A set of research tools for FT-ICR/MS-based metabolomics has been designed exclusively for direct infusion analyses of crude biological samples. Using a series of data processing (the Dr.DMASS program) and a metabolite-species database search (the KNApSACk database), metabolite candidates are assigned to each mass value in FT-ICR/MS spectral data, and statistical analysis is successful in identifying metabolite candidates contributing to the formation of specific metabolic profiles. While the scheme was developed for high-throughput metabolic profiling based on direct infusion analyses, the high potential of the mass resolving power of FT-ICR/MS in MSⁿ analyses can be fully applied when selected metabolites are studied in detail. Based on the Dr.DMASS and the KNApSACk database, an in-house data-processing scheme for LC-coupled FT-ICR/MS metabolomics is under development, focusing on annotation of metabolite candidates to every detectable ion, together with MS–MS fragmentation patterns.

Acknowledgements The authors are grateful to our colleagues for valuable discussions and experiments. This work was performed as one of the technology development projects of the "Green Biotechnology Program" supported by NEDO (New Energy and Industrial Technology Development Organization), Japan. This work was supported in part by the Ministry of Education, Culture, Sports, Science, and Technology of Japan (18380201 and 18038037 to D.O.).

References

1. Fiehn O (2002) *Plant Mol Biol* 48:155–171
2. Sumner L, Mendes P, Dixon R (2003) *Phytochemistry* 62:817–836
3. Schauer N, Fernie AR (2006) *Trends Plant Sci* 11:508–516
4. Soga T, Baran R, Suematsu M, Ueno Y, Ikeda S, Sakurakawa T, Kakazu Y, Ishikawa T, Robert M, Nishioka T, Tomita M (2006) *J Biol Chem* 281:16768–16776
5. Griffin JL (2006) *Curr Opin Chem Biol* 4:309–315
6. Dettmer K, Aronov PA, Hammock BD (2007) *Mass Spectrom Rev* 26:51–78
7. Aranibar N, Singh BK, Stockton GW, Ott KH (2001) *Biochem Biophys Res Commun* 286:150–155
8. Viant MR, Rosenblum ES, Tjeerdema RS (2003) *Environ Sci Technol* 37:4982–4989
9. Choi YH, Tapias EC, Kim HK, Lefeber AWM, Erkelens C, Verhoeven JJJ, Brzin J, Zel J, Verpoorte R (2004) *Plant Physiol* 135:2398–2410
10. Crockford DJ, Holmes E, Lindon JC, Plumb RS, Zirah S, Bruce SJ, Rainville P, Stumpf CL, Nicholson JK (2006) *Anal Chem* 78:363–371
11. Marshall AG, Hendrickson CL, Jackson GS (1998) *Mass Spectrom Rev* 17:1–35
12. Sanders M, Shipkova PA, Zhang H, Warrack BM (2006) *Curr Drug Metab* 7:547–555
13. Payne AH, Glish GL (2005) *Methods Enzymol* 402:109–148
14. Rompp A, Taban IM, Mihalca R, Duursma MC, Mize TH, McDonnell LA, Heeren RM (2005) *Eur J Mass Spectrom* 11:443–456
15. Aharoni A, Ric de Vos CH, Verhoeven HA, Maliepaard CA, Kruppa G, Bino R, Goodenowe DB (2002) *OMICS* 6:217–234
16. Hirai MY, Yano M, Goodenowe DB, Kanaya S, Kimura T, Awazuhara M, Arita M, Fujiwara T, Saito K (2004) *Proc Natl Acad Sci USA* 101:10205–10210
17. Hirai MY, Klein M, Fujikawa Y, Yano M, Goodenowe DB, Yamazaki Y, Kanaya S, Nakamura Y, Kitayama M, Suzuki H, Sakurai N, Shibata D, Tokuhisa J, Reichelt M, Gershenzon J, Papenbrock J, Saito K (2005) *J Biol Chem* 280:25590–25595
18. Tohge T, Nishiyama Y, Hirai MY, Yano M, Nakajima J, Awazuhara M, Inoue E, Takahashi H, Goodenowe DB, Kitayama M, Noji M, Yamazaki M, Saito K (2005) *Plant J* 42:218–235
19. Oikawa A, Nakamura Y, Ogura T, Kimura A, Suzuki H, Sakurai N, Shinbo Y, Shibata D, Kanaya S, Ohta D (2006) *Plant Physiol* 142:398–413
20. Shinbo Y, Nakamura Y, Altaf-Ul-Amin M, Asahi H, Kurokawa K, Arita M, Saito K, Ohta D, Shibata D, Kanaya S (2006) *57:166–181*
21. Kanaya S, Kinouchi M, Abe T, Kudo Y, Yamada Y, Nishi T, Mori H, Ikemura T (2001) *Gene* 276:89–99
22. Abe T, Kanaya S, Kinouchi M, Ichiba Y, Kozuki T, Ikemura T (2002) *Genome Res* 13:693–702
23. Roessner U, Luedemann A, Brust D, Fiehn O, Linke T, Willmitzer L, Fernie AR (2001) *Plant Cell* 13:11–29
24. Steinrücken HC, Amrhein N (1980) *Biochem Biophys Res Commun* 94:1207–1212
25. Smith IK (1985) *Plant Physiol* 79:1044–1047
26. Jain M, Bhalla-Sarin N (2001) *Pestic Biochem Physiol* 69:143–152
27. Marrs KA (1996) *Annu Rev Plant Physiol Plant Mol Biol* 47:127–158
28. Rea PA, Li ZS, Lu YP, Drozdowicz YM, Martinoia E (1998) *Annu Rev Plant Physiol Plant Mol Biol* 49:727–760
29. Tausz M, Sircelj H, Grill D (2004) *J Exp Bot* 55:1955–1962